

# G<sub>1</sub> Cell Cycle Arrest Is Induced by the Fourth Extracellular Loop of Meningococcal PorA in Epithelial and Endothelial Cells

Vassey, Matthew; Firdaus, Rininta; Aslam, Akhmed; Wheldon, Lee M.; Oldfield, Neil J.; Ala'Aldeen, Dlawer A. A.; Wooldridge, Karl G.

DOI:  
[10.1155/2023/7480033](https://doi.org/10.1155/2023/7480033)

License:  
Creative Commons: Attribution (CC BY)

*Document Version*  
Publisher's PDF, also known as Version of record

*Citation for published version (Harvard):*  
Vassey, M, Firdaus, R, Aslam, A, Wheldon, LM, Oldfield, NJ, Ala'Aldeen, DAA & Wooldridge, KG 2023, 'G<sub>1</sub> Cell Cycle Arrest Is Induced by the Fourth Extracellular Loop of Meningococcal PorA in Epithelial and Endothelial Cells', *Cellular Microbiology*, vol. 2023, 7480033. <https://doi.org/10.1155/2023/7480033>

[Link to publication on Research at Birmingham portal](#)

## General rights

Unless a licence is specified above, all rights (including copyright and moral rights) in this document are retained by the authors and/or the copyright holders. The express permission of the copyright holder must be obtained for any use of this material other than for purposes permitted by law.

- Users may freely distribute the URL that is used to identify this publication.
- Users may download and/or print one copy of the publication from the University of Birmingham research portal for the purpose of private study or non-commercial research.
- User may use extracts from the document in line with the concept of 'fair dealing' under the Copyright, Designs and Patents Act 1988 (?)
- Users may not further distribute the material nor use it for the purposes of commercial gain.

Where a licence is displayed above, please note the terms and conditions of the licence govern your use of this document.

When citing, please reference the published version.

## Take down policy

While the University of Birmingham exercises care and attention in making items available there are rare occasions when an item has been uploaded in error or has been deemed to be commercially or otherwise sensitive.

If you believe that this is the case for this document, please contact [UBIRA@lists.bham.ac.uk](mailto:UBIRA@lists.bham.ac.uk) providing details and we will remove access to the work immediately and investigate.

## Research Article

# G<sub>1</sub> Cell Cycle Arrest Is Induced by the Fourth Extracellular Loop of Meningococcal PorA in Epithelial and Endothelial Cells

Matthew Vassey, Rininta Firdaus , Akhmed Aslam, Lee M. Wheldon, Neil J. Oldfield, Dlawer A. A. Ala'Aldeen, and Karl G. Wooldridge 

Molecular Bacteriology and Immunology Group, School of Life Sciences, University of Nottingham, UK

Correspondence should be addressed to Karl G. Wooldridge; [karl.wooldridge@nottingham.ac.uk](mailto:karl.wooldridge@nottingham.ac.uk)

Matthew Vassey and Rininta Firdaus contributed equally to this work.

Received 19 June 2022; Revised 11 December 2022; Accepted 14 December 2022; Published 28 March 2023

Academic Editor: Jayaprakash Kolla

Copyright © 2023 Matthew Vassey et al. This is an open access article distributed under the Creative Commons Attribution License, which permits unrestricted use, distribution, and reproduction in any medium, provided the original work is properly cited.

*Neisseria meningitidis* is the most frequent cause of bacterial meningitis and is one of the few bacterial pathogens that can breach the blood-brain barrier (BBB). The 37/67 kDa laminin receptor (LamR) was previously identified as a receptor mediating meningococcal binding to rodent and human brain microvascular endothelial cells, which form part of the BBB. The meningococcal surface proteins PorA and PilQ were identified as ligands for this receptor. Subsequently, the fourth extracellular loop of PorA (PorA-Loop4) was identified as the LamR-binding moiety. Here, we show that PorA-Loop4 targets the 37 kDa laminin receptor precursor (37LRP) on the cell surface by demonstrating that deletion of this loop abrogates the recruitment of 37LRP under meningococcal colonies. Using a circularized peptide corresponding to PorA-Loop4, as well as defined meningococcal mutants, we demonstrate that host cell interaction with PorA-Loop4 results in perturbation of p-CDK4 and Cyclin D1. These changes in cell cycle control proteins are coincident with cellular responses including inhibition of cell migration and a G<sub>1</sub> cell cycle arrest. Modulation of the cell cycle of host cells is likely to contribute to the pathogenesis of meningococcal disease.

## 1. Introduction

Many bacterial pathogens have developed strategies to subvert, evade, or modulate host cell responses to promote their own survival and replication [1]. These effects are mediated by a diverse array of toxins, surface proteins, and other effector molecules [2].

Bacterial surface components are paramount in the interaction of bacteria with host cells, especially in the contexts of pathogenesis and immunity. In Gram-negative bacteria, major outer membrane proteins (OMPs), including porins, play fundamental roles in bacterial function and pathogenicity [3, 4].

We previously identified the 37/67 kDa laminin receptor (LamR) as a common receptor targeted by three important bacterial pathogens capable of causing meningitis: *Strepto-*

*coccus pneumoniae*, *Haemophilus influenzae*, and *Neisseria meningitidis* [5]. We demonstrated that the bacterial ligands were pneumococcal CbpA, meningococcal PilQ and PorA, and OmpP2 of *H. influenzae*. Very recently, Lithgow et al. showed that LamR is also targeted by the neuroinvasive pathogen *Treponema pallidum*, suggesting a common mechanism for penetration of the blood-brain barrier by invasive bacterial pathogens [6].

Meningococcal PorA and *H. influenzae* OmpP2 are abundant, multifunctional outer membrane proteins belonging to the porin family; despite displaying only limited sequence similarity, they share many structural characteristics and both play fundamental roles in bacterial adhesion and invasion [5, 7]. Bacterial porins are pore-forming proteins localized to the outer membrane as stable homotrimeric complexes that form water-filled channels [8]. Porin

TABLE 1: Amino acid sequences of synthetic extracellular loop peptides used in this study.

Peptide name	Amino acid sequence
PorA-Loop4	CPIQNSKSAYTPAYYTKNTNNTLTPAVVVGKPGSC
ScLoop4	CNSNGATGKNPPVVTLKKSIVYQSNYTPAYANTILPC

monomers each cross the outer membrane as a series of 16  $\beta$ -strands forming a  $\beta$ -barrel structure with eight loops of varying length exposed on the outer surface [8]. The roles of these surface-exposed loops are of considerable interest, and numerous studies have shown their importance in terms of host-pathogen interactions [3]. In particular, extracellular loops have been shown to bind specific cellular receptors, to mediate signalling, and to modulate the immune response [9–13].

OmpP2 of *H. influenzae* is one of the best characterized porins in terms of its host-pathogen interactions. OmpP2 induces activation of signalling pathways through the MEK1-MEK2/MAPK cascade [14]. A synthetic peptide corresponding to extracellular Loop7 of OmpP2 is responsible for activation of MEK1/MEK2/MAPK signalling pathways, and interaction induced key pathophysiological changes including modification of circulating markers of endothelial injury: changes that have significant consequences for bacterial sepsis [15, 16].

Compared to OmpP2, less is known about the contribution of meningococcal PorA to host-pathogen interactions. The most significant sequence variation within PorA occurs within the first, fourth, and fifth extracellular loops of this porin (variable regions 1, 2, and 3, respectively) [17, 18]; this variability is the basis for meningococcal sero-subtyping [19, 20].

Previously, we investigated the role of PorA extracellular loops in LamR binding and revealed that the fourth extracellular loop mediates this interaction [21]. The aims of this study were to determine the species of LamR receptor on the cell surface to which PorA binds as this receptor exists in multiple forms. Furthermore, we aimed to determine how LamR binding by PorA affects the behavior of the infected cell. We show that a circularized synthetic peptide corresponding to PorA-Loop4 mediates binding to the host cell via the 37 kDa laminin receptor “precursor” in preference to the 67 kDa “mature” form of this receptor. The addition of this peptide to epithelial and endothelial cells initiates significant changes to these cells including inhibition of cell migration and induction of  $G_1$  cell cycle arrest. The role of PorA-Loop4 was confirmed using intact meningococcal cells expressing either wild-type PorA or a mutant derivative of PorA lacking the fourth extracellular loop.

## 2. Materials and Methods

**2.1. Bacterial Strains, Mutants, and Culture Conditions.** *Neisseria meningitidis* strain MC58 was obtained from the American Type Culture Collection. The PorA deletion mutant of MC58 (MC58  $\Delta$ PorA) and the PorA-Loop4 deletion mutant (MC58  $\Delta$ PorA-Loop4) have been described previously [5, 21]. All meningococcal strains were grown at 37°C, in an atmosphere of air plus 5% CO<sub>2</sub>, on Columbia agar with chocolate horse blood (Oxoid) or in brain heart

infusion (BHI) broth (Oxoid) supplemented, where appropriate, with streptomycin and spectinomycin (each at 100  $\mu$ g ml<sup>-1</sup>).

**2.2. Synthetic Peptides.** The synthetic PorA-Loop4 peptides utilized in this study are detailed in Table 1. Both were synthesized by Alta Bioscience, UK, and were high purity grade (peptide purity > 95%). Additional terminal cysteine residues were incorporated into both peptides to facilitate cyclisation via disulfide bond formation to simulate the cell-surface loop structure.

**2.3. Cell Association and Cell Invasion Assay.** Cell association and invasion assays were performed as described previously [22]. HBMEC monolayers (10<sup>6</sup> cells) in 6-well plates were infected with bacteria at a multiplicity of infection (MOI) of 500 and left to associate for 2–8 h at 37°C, 5% CO<sub>2</sub>. Starting inoculums were retrospectively confirmed by serial dilution and plating. To assess association of meningococcal cells with the HBMECs, the monolayers were washed four times with PBS. The cells were then disrupted and homogenized in 1 ml 0.1% saponin in PBS. Meningococci were enumerated by serial dilution and plating of the suspension onto chocolate agar plates. Colony forming unit (cfu) was determined by plating 10  $\mu$ l spots from the diluted suspensions. To enumerate invasion of HBMEC monolayers by meningococcal cells, the same procedure was followed except that, after washing of the infected monolayers, the medium was replaced with Endoprime medium containing gentamicin (100  $\mu$ g ml<sup>-1</sup>) and incubating for a further hour before the wells were processed as described above for cell association.

**2.4. Cell Culture.** Human brain microvascular endothelial cells (HBMECs; ScienCell Research Labs) were cultured in Endoprime media supplemented with 5% (v/v) fetal bovine serum (FBS), IGF, bFGF, ascorbic acid, hydrocortisone and heparin, EGF, VEGF (all from PAA), 100 U ml<sup>-1</sup> penicillin, and 100  $\mu$ g ml<sup>-1</sup> streptomycin (Gibco). Cells were immortalized cells at P10–30 passage. Detroit 562 nasopharyngeal epithelial cells (ATCC CCL-138) were cultured in Eagle’s minimum essential medium supplemented with 100 U ml<sup>-1</sup> penicillin and 100  $\mu$ g ml<sup>-1</sup> streptomycin (Gibco) and 10% (v/v) FBS. HCT116 epithelial cells (ATCC CCL-247) were grown in Dulbecco’s modified Eagle’s medium (DMEM, Invitrogen) supplemented with 100 U ml<sup>-1</sup> penicillin and 100  $\mu$ g ml<sup>-1</sup> streptomycin (Gibco) and 10% (v/v) FBS. Cells were maintained at 37°C, 5% CO<sub>2</sub>. Cell culture medium was changed every 2 days, and cells were split using trypsin-EDTA (Gibco) upon reaching 90% confluence. Where cells were routinely cultured on fibronectin, fibronectin-coated T75 flasks were used (BD Biosciences).

**2.5. EdU Cell Proliferation Assay.** The quantification of 5-ethynyl-2'-deoxyuridine (EdU) incorporation into the S-phase (during active DNA replication) was performed using the Click-iT EdU Flow Cytometry Assay Kit (Invitrogen) according to the manufacturer's instructions. Briefly, non-confluent cells were treated with PorA-Loop4 (or controls) and incubated for 24 h. The cells were then labeled with 20  $\mu$ M EdU for 2 h. After labeling with EdU, the cells were fixed and permeabilized, and Click-iT<sup>®</sup> EdU antibody with Alexa Fluor 488 was added. Cells were counterstained with DAPI (Invitrogen) for 1 h at room temperature before being mounted onto microscope slides with ProLong Gold antifade. EdU incorporation was determined using confocal microscopy by quantifying the number of cells that had incorporated EdU relative to the untreated controls.

**2.6. Cell Cycle Analysis.** We utilized the widely used assay to analyze the cell cycle using 5-bromo-2'-deoxyuridine (BrdU) [23]. Cells were seeded into 6 well tissue culture plates (Corning), at approximately 60% confluency. Cells were treated with proteins, peptides, or controls and incubated for 24 h. At 22 h post-treatment, BrdU (final conc. 20  $\mu$ M; Sigma-Aldrich) was added to each well and incubated for a further 2 h at 37°C. Cells were washed with PBS before detachment with trypsin/EDTA (1 $\times$ ) solution (Gibco). Cells were then washed again and fixed with ice cold 70% ethanol. After fixing, cells were washed twice in PBS and then incubated with 2 M HCl. After washing once in PBS, this was followed by two washes in PBS-T/BSA. Cell pellets were resuspended in 50  $\mu$ l PBS-T/BSA and stained with FITC-conjugated anti-BrdU antibody (BD Bioscience) as per the manufacturer's instructions. Cells were washed once with PBS and resuspended in PBS. Finally, 10  $\mu$ l RNaseA (final concentration 10  $\mu$ g ml<sup>-1</sup>) and 1  $\mu$ l propidium iodide (PI; final concentration 1  $\mu$ g ml<sup>-1</sup>; Sigma) were added to each tube, and tubes were stored in the dark prior to analysis. To determine the population of cells in each phase of the cell cycle, data was acquired using a BD FACSaria (Becton Dickinson) flow cytometer; and in each case, a minimum of 10,000 cells were counted in duplicate for each experiment. Data analysis was carried out, using WinMDI Version 2.9, on a minimum of three independent experiments. Briefly, cells were gated to remove cellular debris, and then, subsequent cells were subjected to pulse processing to determine G<sub>1</sub>-doublets. Once gated, cells were gated based on positive FITC staining and PI staining.

**2.7. Migration Assay.** The migration ability of epithelial cells exposed to PorA-Loop4 peptide was assessed using a classic scratch wound assay, which measures the migration of a cell population as a monolayer [24]. HCT116 epithelial cells (2  $\times$  10<sup>5</sup> cells ml<sup>-1</sup>) were cultured with DMEM medium containing 10% FBS in 12-well plates previously treated with fibronectin (1.6  $\mu$ g cm<sup>-2</sup>) to nearly confluent cell monolayers. Prior to the migration experiment, an XTT-based cytotoxicity assay demonstrated that none of the synthetic peptides used in the study had an adverse effect on HCT116 or HBMEC cell viability. An artificial linear wound (scratch) was then introduced using a 200  $\mu$ l sterile pipette tip the full

length of the well. The cells were rinsed with DMEM to remove the cellular debris, and the media was replaced with DMEM containing 10% FBS  $\pm$  peptide treatment. Immediately after treatment, scratched areas were imaged using a Nikon Eclipse TE2000-S microscope with a Hamamatsu digital camera. This was connected to a computer where images were captured using IP Lab image software (Version 1.6). All wounds were visualized and recorded at 0, 16, 24, 40, and 60 h, and cellular migration into the wounded area was quantified using ImageJ (version 1.45 s). The same position on the wound was imaged each time, and five measurements were taken across each frame. Results were expressed as percentage cell migration after treatment in comparison to the control group at each time point.

**2.8. Meningococcal Colocalization Assay.** Fresh overnight cultures of *N. meningitidis* MC58 strains were inoculated into cell culture media (Endoprime media (PAA—supplemented with IGF, bFGF, ascorbic acid, hydrocortisone and heparin, EGF, VEGF, and 5% FBS (v/v))) and incubated until the OD at 600 nm reached 0.5. HBMEC cells were cultured as described above in 24-well tissue culture plates (Costar) containing acid-etched coverslips pretreated with bovine fibronectin (1.6  $\mu$ g/cm<sup>2</sup>). Prior to all colocalization assays, cells were washed twice in antibiotic-free media. For colocalization assays, cell monolayers were infected with 1  $\times$  10<sup>7</sup> cfu of *N. meningitidis* MC58 strains (MOI of ca. 300) and left to associate for 2 h. After association, cells were washed and then fixed with 4% paraformaldehyde (PFA). Coverslips were then washed in preparation for immunofluorescent staining.

**2.9. Immunoblotting and Densitometry Analysis.** Cells were lysed with radio-immunoprecipitation assay (RIPA; Sigma-Aldrich) buffer (supplemented with PhosSTOP (Merck Millipore) and c0mplete Mini EDTA-free protease inhibitor cocktail (Roche)) for 30 min on ice. Samples were run on 10% gradient SDS-PAGE gels (Thermo-Scientific) calibrated with ColorPlus prestained markers (NEB). Gels were transferred to nitrocellulose membrane (BioRad) on a Trans-Blot<sup>®</sup> semi-dry transfer system. Membranes were blocked (TBS-T/5% BSA, 1 h at RT). Primary antibodies (in TBS-T/5% BSA) were incubated with the membrane overnight at 4°C. Membranes were washed in TBS-T and then probed with conjugated secondary antibody (in TBS-T/5% BSA, 1 h at room temperature). The membrane was washed again, before membranes were exposed to Luminata<sup>™</sup> Crescendo Western HRP Substrate (Millipore) for 5 min. The membranes were drained and scanned with a C-Digit Blot Scanner (LI-COR Biosciences) to visualize immunoreactive proteins. Reactive bands in the scanned blots were quantified with ImageJ software. The area of each band was compared to the untreated sample (relative density). Then, the relative density of each sample was compared to the relative density of the loading control (adjusted density/fold change).

**2.10. Immunofluorescence.** Cells were grown on acid-etched 12 mm coverslips (SLS) and coated with bovine fibronectin (1  $\mu$ l cm<sup>-2</sup>) as required. Following treatment, cells were fixed

TABLE 2: List of primers used for qRT-PCR experiments in this study.

Gene of interest	Forward primer	Reverse primer
GAPDH	CAACGTGTCAAGTGGTGGACC	CCTGCTTCACCACCTTCTTG
Cyclin D1	CCGTCCATGCGGAAGATC	GAAGACCTCCTCCTCGCACT
CDK4	AGTGTGAGAGTCCCAATGG	CGAACTGTGCTGATGGGAAG

(4% paraformaldehyde (PFA), 10 min at room temperature) and permeabilized as required (0.1% Triton™ X-100/1% BSA in PBS). Following blocking (PBS/4% BSA), samples were incubated with primary antibody(s) (in PBS-T/4% BSA) either as a cocktail or sequentially: anti-67 kDa LamR1 (MAb MLuC5, 1:100, Abcam) and anti-37 kDa LamR1 MAb A7, 1:250 (Santa Cruz Biotech). The following 3 washes in PBS samples were incubated with conjugated secondary antibody(s) (in PBS-T/4% BSA): antimouse IgM (Alexa647, 1:1500; Alexa488, 1:1000), antimouse IgG (Alexa680, 1:200), and antirabbit (Alexa488, 1:400; Alexa680 1:200), all from Molecular Probes. Following three washes in PBS, one in dH<sub>2</sub>O, samples were mounted with ProLong Gold antifade with DAPI (Invitrogen). For each experiment, unstained and secondary antibody alone samples were processed in parallel to control for non-specific staining. Additionally, all primary/secondary combinations were checked for cross-reactivity and sequential staining used as required. For colocalization studies, samples stained for localization of each protein individually were processed in parallel. In all cases, adjacent channels were monitored for bleed-through.

**2.11. Confocal Microscopy.** Images (400 nm optical sections unless otherwise stated) were acquired with a Zeiss LSM 700 Axio Observer using a Plan-Apochromat 63×/1.40 Oil DIC M27 objective. Images were processed using ImageJ and Adobe Photoshop software. Confocal raw data are available upon request. Colocalization analyses utilized the ZEN software function with a FI threshold of 50 and are not intensity-weighted. Mean FI data of individual cells or fields were also obtained using ZEN software.

**2.12. qRT-PCR.** Cells were washed twice with serum-free Endoprime base media and total RNA extracted using the RNA easy mini kit (Qiagen) according to the manufacturer's instructions. DNA was removed using RNAase-free TurboDNase I (Ambion, Applied Biosystems). RNA was cleaned and concentrated using RNeasy MinElute Cleanup Kit (Qiagen). cDNA was synthesized using High-Capacity cDNA Reverse Transcription Kit (Thermo Fisher Scientific). qRT-PCR was performed in an ABI7500 Real-Time PCR System (Applied Biosystems) with Power SYBR® Green PCR Master Mix (Applied Biosystems) according to the manufacturer's instructions. Primers specific to CDK4, Cyclin D1, and GAPDH were used for amplification of 59, 75, and 80 bp fragments, respectively (Table 2). To test PCR efficiency, a standard curve was generated with serial ten-fold dilution of a known amount of HBMEC cDNA using 100 nM of forward and reverse primers. A standard curve was plotted for GAPDH, CDK4, and Cyclin D1 using template dilution ver-

sus  $C_T$  and  $\Delta C_T$  values. The qPCR reaction mixture (10  $\mu$ l total volume) consisted of 1  $\mu$ l of cDNA (50 ng  $\mu$ l<sup>-1</sup>), 5  $\mu$ l Power SYBR® Green PCR Master Mix (2×), 100 nM forward and reverse primer, and H<sub>2</sub>O. Cycling was initiated at 95°C for 2 min, followed by 40 cycles of 95°C for 15 s and 60°C for 60 s. Samples were run in triplicate and relative expression of CDK4, and Cyclin D1 was normalized to GAPDH as housekeeping gene. The quantification of CDK4 and Cyclin D1 expression was calculated relative to untreated HBMECs and was determined by the  $\Delta\Delta C_T$  method [25].

**2.13. Statistical Analysis.** Where values from 2 experimental conditions were compared, we used a 2-tailed Student's *t*-test to test for significance. Where multiple experimental conditions were compared with a single control group, statistical significance was tested using 1-way ANOVA. A Dunnett's test was applied post hoc to validate significance of data against the untreated control group. A *P* value less than 0.05 was considered statistically significant, while *P* values less than 0.01 were considered highly statistically significant. All statistical analysis was carried out using Prism GraphPad (Version 6.04 for Windows).

### 3. Results

**3.1. *Neisseria meningitidis* Recruits the 37 kDa Laminin Receptor Precursor and This Is Mediated by Extracellular Loop4 of the Outer Membrane Protein PorA.** Previously, we showed that meningococcal PorA interacts with LamR *in vitro* and *in vivo* via its fourth extracellular loop (PorA-Loop4) [21]. Furthermore, in ELISA assays, we showed that a synthetic circularized peptide corresponding to PorA-Loop4 bound to the recombinant laminin receptor [21]. The laminin receptor is known to be present on the cell surface in two distinct forms: the 37 kDa "laminin receptor precursor" (37LRP) and a 67 kDa "laminin receptor" (67LR). To determine which receptor species PorA interacts with, commercially available antibodies were used to identify the different LamR species in human brain microvascular endothelial cells (HBMEC) and observe how their cellular localization changed in response to the presence of PorA-Loop4.

HBMECs were infected with the wild-type *N. meningitidis* strain MC58 for 2 h. Cells were then analyzed by confocal microscopy to quantify the colocalization coefficient of the meningococcal colonies with 37LRP or 67LR. Both isoforms were observed on the surface of uninfected HBMECs (Figure S1), and while the bacteria colocalized with both receptor species, they were found to colocalize to a small but significantly greater extent with 37LRP than with 67LR (71% and 58%, respectively; Figures 1(a)

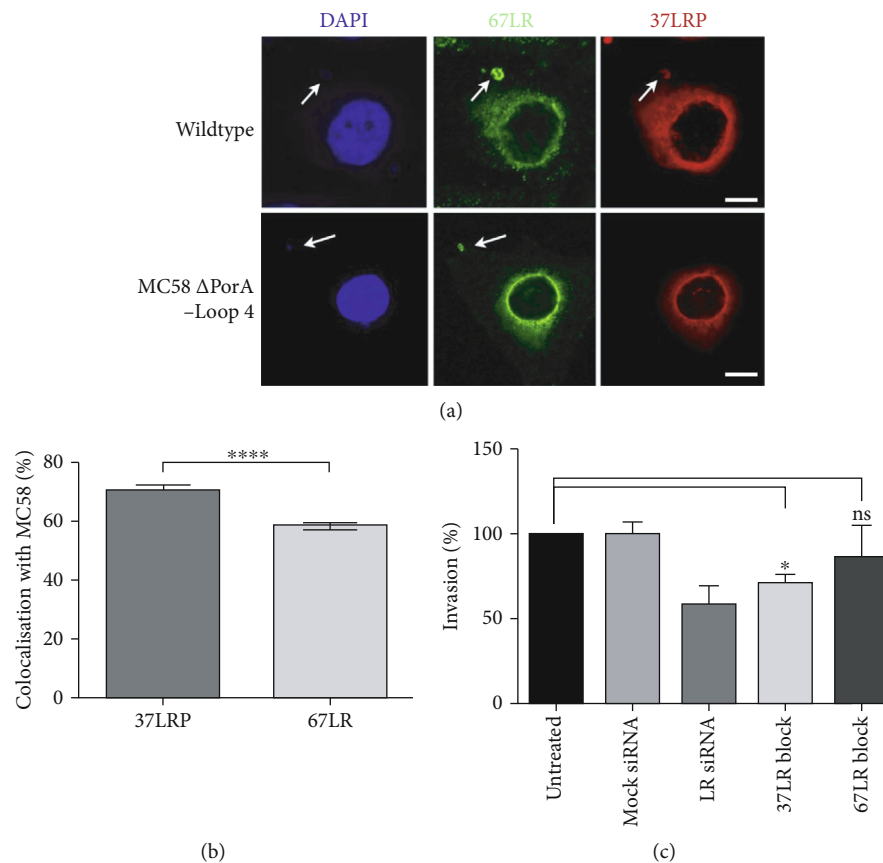


FIGURE 1: *Neisseria meningitidis* recruits the 37 kDa laminin receptor precursor and this is mediated by extracellular Loop4 of the outer membrane protein PorA. (a) HBMECs were infected with either wild-type *N. meningitidis* MC58 or its isogenic derivative MC58  $\Delta$ PorA-Loop4 and fixed and stained to measure colocalization of 37LRP (red) and 67LR (green) with bacterial colonies (stained with DAPI; blue). Representative confocal images are shown; white arrow indicates a meningococcal colony on the cell surface. Scale bar represents 20  $\mu$ m. (b) Colocalization coefficient (%) of *N. meningitidis* MC58 wild-type microcolonies with either 37LRP (black bar) or 67LR (grey bar) (\*\*\*\* $P$  value  $\leq 0.001$ ;  $t$ -test). (c) The effect of LamR siRNA treatment or antibody inhibition on the invasion of *N. meningitidis* MC58 into HBMECs. Prior to infection, cells were treated with either nontargeting siRNA or LamR siRNA (for 48 h), or monoclonal antibody directed towards a specific LamR population for one hour (A7 for 37LRP or Mluc5 for 67LR; both at 25  $\mu$ g ml<sup>-1</sup>). The number of bacteria per cell was determined by counting colony-forming units after overnight incubation. Bacterial invasion is expressed as a percentage normalized to the untreated control. Assays were carried out in triplicate in three independent experiments (\* $P \leq 0.05$ ; one-way ANOVA with Dunnett's test applied post hoc).

and 1(b);  $P > 0.001$ ). Additionally, preincubation of HBMECs with 37LRP-specific antibody significantly reduced invasion of wild-type *N. meningitidis* strain MC58, whereas the 67LR-specific antibody had no such effect (Figure 1(c)).

HBMECs were infected with either wild-type *N. meningitidis* strain MC58 or an isogenic mutant in which Loop4 was deleted ( $\Delta$ PorA-Loop4). The wild-type and the mutant were previously confirmed by immunoblotting with antibody specific for Loop4 (Figure S2). Quantification of the colocalization coefficient showed that recruitment of 67LR to *N. meningitidis* MC58 was not affected by deletion of PorA-Loop4 (Figure S3, left panel). However, the ability of this mutant to colocalize with 37LRP was significantly reduced (Figure S3, right panel).

**3.2. Migration of Epithelial Cells Is Inhibited by PorA-Loop4 Peptide.** The laminin receptor is well documented as being an important receptor for host cell binding to the extracellular

matrix. We hypothesized that binding of PorA-Loop4 to the laminin receptor may interfere with cell adhesion and migration.

The ability of PorA-Loop4 to inhibit cell migration was measured using a wound healing "scratch" assay [24]. After creating a wound in an epithelial (HCT116) cell monolayer and treating with PorA-Loop4 peptide at 5 or 50  $\mu$ M, or scrambled PorA-Loop4 peptide (PorA-Scr Loop4) at 50  $\mu$ M, the wound was monitored over a 60 h time-course during which the gap created by the scratch was closed in untreated monolayers.

PorA-Loop4 was observed to inhibit wound repair at both concentrations tested (Figure 2). PorA-Loop4 at the higher concentration was able to significantly inhibit cell migration at all timepoints between 16 and 60 hours compared to the untreated control ( $P > 0.05$ , 1-way ANOVA). However, PorA-Loop4 at the lower concentration (5  $\mu$ M) was only able to inhibit cell migration up to 40 h.

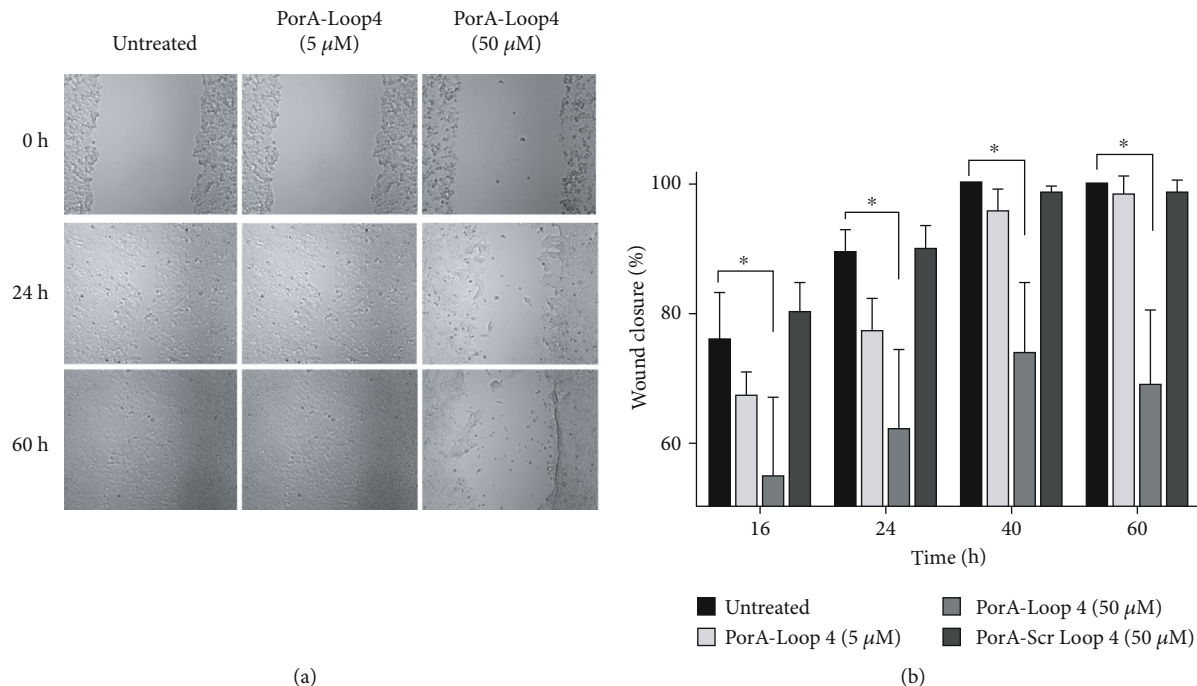


FIGURE 2: Migration of epithelial cells is inhibited by PorA-Loop4 peptide. HCT116 cell monolayers were mechanically wounded, treated, and wound closure monitored over a 60 h time course. (a) Representative light microscope images showing wound closure following treatment with media only (untreated), or PorA-Loop4 (at 5 μM or 50 μM final conc.) at 0, 24, and 60 h. (b) Percentage wound closure of epithelial cells treated with PorA-Loop4 (at 5 μM or 50 μM final conc.) or a scrambled Loop4 peptide (PorA-Scr Loop4; at 50 μM). Wound width was determined by measuring 5 different points across the same field of view on the same wound at each time point. All data are normalized to the time 0 wound width and expressed as mean percentage (%) wound closure (+ SEM) from three independent experiments, each carried out in triplicate. \*Significantly different compared to untreated (\* $P \leq 0.05$ : one-way ANOVA with Dunnett's test applied post hoc).

Representative images of untreated controls and PorA-Loop4 treated cells at 0, 24, and 60 h are shown in Figure 2(a). Wound healing was quantified for untreated cells, cells treated with PorA-Loop4 at either concentration, or PorA-Scr Loop4 at the higher concentration (Figure 2(b)). Cells treated with PorA-Scr Loop4 migrated and closed the wound between 24 and 40 h with no significant difference to the untreated controls (Figure 2(b)).

**3.3. PorA-Loop4 Causes a Decrease in the Proportion of Cells Transitioning into S-Phase.** Engagement of the laminin receptor by some ligands has been shown to affect the host cell cycle [26], and infection by meningococci can prevent cell migration: an effect that is independent of type IV pili [24]. Here, we investigated whether treatment of epithelial or endothelial cells with PorA-Loop4 could affect DNA synthesis and the host cell cycle. HBMEC and epithelial cell lines HCT116 and Detroit 562 were treated for 24 h prior to staining for newly synthesized DNA. To quantify the number of cells in S-phase, we utilized a fluorescence microscopy-based method whereby the modified thymidine analog EdU is incorporated into newly synthesized DNA using Click-iT chemistry. Alexa Fluor® was used to fluorescently label the incorporated EdU in DAPI-stained cells. The number of cells actively entering S-phase relative to the total cell population was then determined. All three cell types showed a significant decrease in the number of cells

in S-phase in response to treatment with PorA-Loop4. Treatment with PorA-Loop4 reduced the number of cells in S-phase by 24%, 10%, and 11% in HBMECs, HCT116, and Detroit 562 cells, respectively (Figure 3 and Figure S4). This effect was comparable with the decrease in the numbers of S-phase cells observed after treatment with nocodazole (used as a positive control) compared to the untreated controls. No significant reduction in the numbers of S-phase cells was observed in cells of any of the cell lines treated with PorA-Scr Loop4 (Figure 3).

**3.4. PorA-Loop4 Causes an Increase in the Proportion of Cells in G<sub>1</sub> Phase.** A reduction in the number of cells newly synthesizing DNA (S-phase) in response to treatment with PorA-Loop4 suggests that the cells may have entered a cell cycle arrest. BrdU incorporation and propidium iodide (PI) costaining was employed to identify the proportions of cells at each cell cycle checkpoint and to identify at what point in the cell cycle the arrest was taking place. BrdU, a modified nucleoside analog, was used to quantify the newly synthesized DNA and PI was employed to costain cell nuclei. Cells were then quantified by flow cytometry. PI is a fluorescent molecule that intercalates in DNA and is used to quantify DNA content and to differentiate between G<sub>1</sub> and G<sub>2</sub>/M. HBMECs, HCT116, and Detroit 562 cells were all treated for 24 h prior to harvesting, and BrdU was added for the final 2 h (at 22 h post-treatment). The BrdU

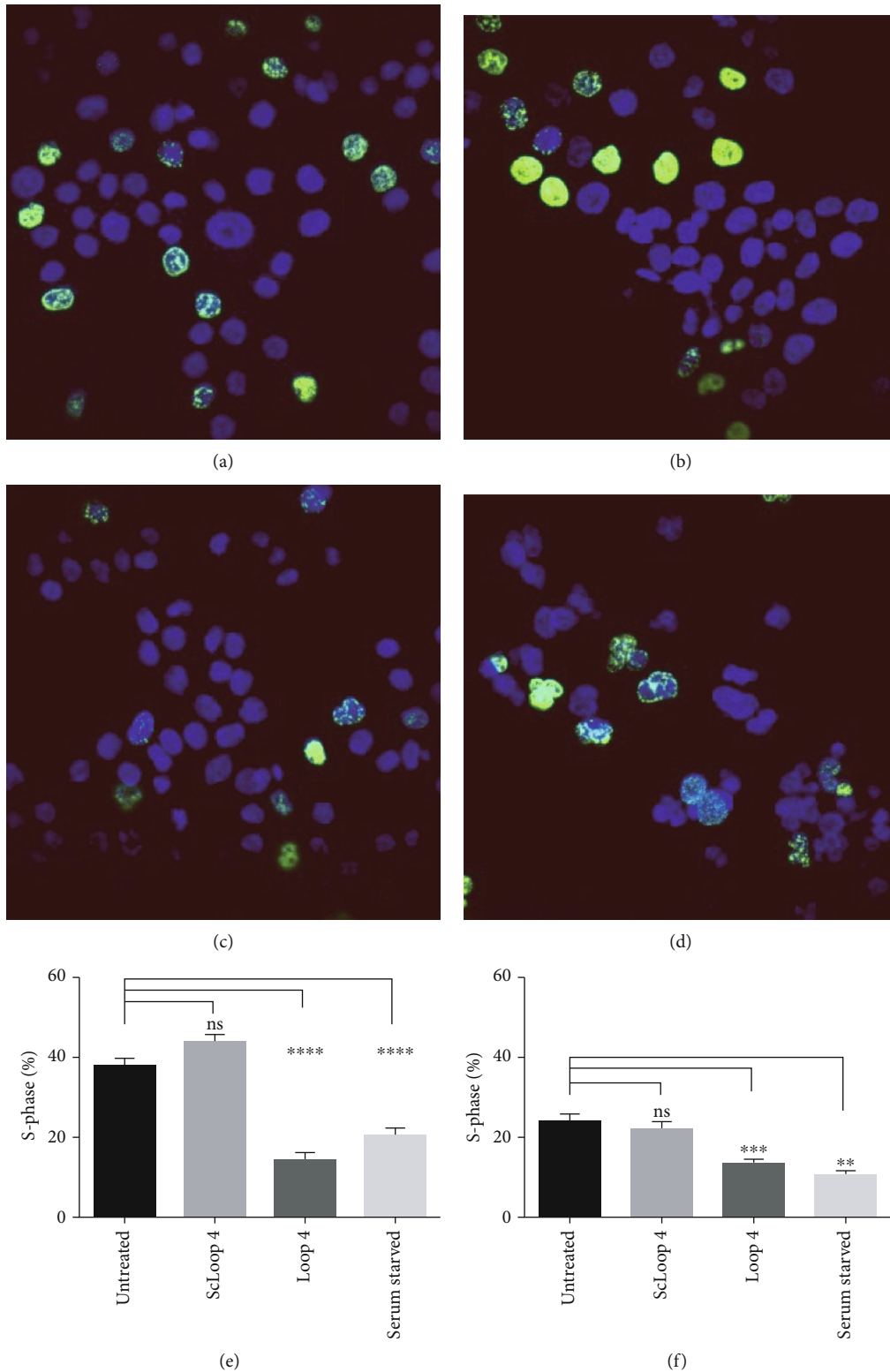


FIGURE 3: PorA-Loop4 causes a decrease in the proportion of cells transitioning into S-phase. HCT116 cells were treated for 24 h. During the final 2 h of incubation, 20  $\mu\text{M}$  of Edu was added and incorporated into S-phase cells. Representative images of (a) untreated, (b) cells treated with PorA-Scr Loop4 (50  $\mu\text{M}$ ), (c) PorA-Loop4 (50  $\mu\text{M}$ ), or (d) nocodazole (0.1  $\mu\text{g ml}^{-1}$ ). Cells were washed, fixed, and stained with DAPI (blue) and anti-EdU antibody (green) and analyzed by confocal microscopy. Percentage of S-phase HBMEC (e) or HCT116 (f) cells (EdU + labeled cells) expressed as a percentage of the total cell number (as determined by DAPI staining). Bars represent the mean + SEM of 30 fields per treatment from three independent experiments. Significant difference compared to untreated (\*\* $P \leq 0.01$ , \*\*\* $P \leq 0.001$ , and \*\*\*\* $P \leq 0.0001$ ; ANOVA with Dunnett's test applied post hoc). Scale bar = 50  $\mu\text{m}$ .



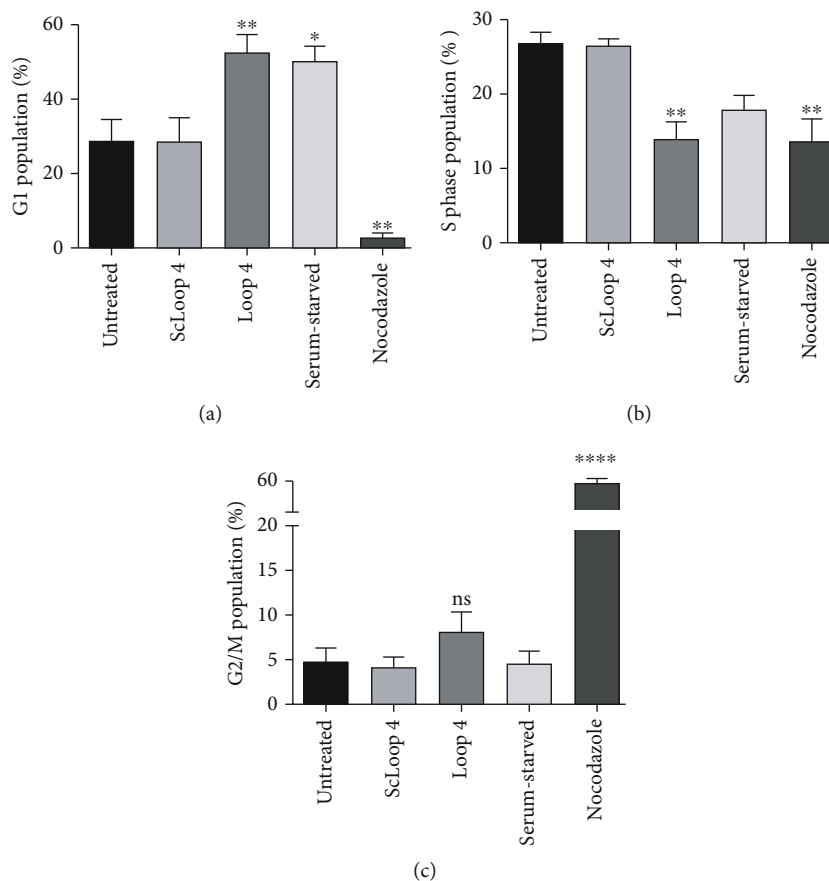


FIGURE 4: PorA-Loop4 causes an increase in the proportion of cells in G<sub>1</sub> phase. HBMECs were treated with either PorA-Loop4 (50  $\mu$ M), PorA-Scr Loop4 (50  $\mu$ M), and nocodazole (50  $\mu$ g ml<sup>-1</sup>) or were serum deprived for 24 h. During the final 2 h of incubation, 20  $\mu$ M of BrdU was added to all cells. Cells were harvested, fixed, and costained with anti-BrdU (Alexa 488) and PI and analyzed for cell cycle by flow cytometry. Proportions of cell cycle phases (a) G<sub>1</sub>, (b) S-phase, and (c) G<sub>2</sub>/M are expressed as percentage of total population for treated cells. Each bar represents at least three independent experiments, and each experiment measured a minimum 10,000 events. Significant difference compared to untreated (\*\* $P \leq 0.01$ , \*\*\* $P \leq 0.001$ , and \*\*\*\* $P \leq 0.0001$ ; ANOVA with Dunnett's test applied post hoc).

incorporation assay confirmed the findings of the previous experiment (using Click-iT chemistry) and showed a significant reduction in the S-phase cell population in PorA-Loop4-treated cells compared to untreated controls. Additionally, a significant increase in the percentage of PorA-Loop4-treated cells was observed at the G<sub>1</sub> checkpoint: >50% more HBMEC cells were observed in G<sub>1</sub> phase after treatment with PorA-Loop4 (Figure 4(a)); significantly fewer cells were observed in PorA-Loop4 and were in S-phase (Figure 4(b)), while the G<sub>2</sub>/M phase population was not significantly affected by PorA-Loop4 treatment (Figure 4(c)). Smaller, but significant increases of PorA-Loop4-treated Detroit 526 and HCT116 cells were observed in G<sub>1</sub> phase: increases of 17% and 12% of these cells, respectively, were arrested at this stage in the cell cycle (Table S1). These observations are consistent with a classic G<sub>1</sub> arrest. There was no significant change in the percentage of cells in the G<sub>2</sub>/M cell population in any cell line tested. Serum starvation (positive control for G<sub>1</sub> arrest) and nocodazole (positive control for G<sub>2</sub>/M arrest) both showed significant cell cycle inhibition at their respective checkpoints compared to untreated controls. PorA-Scr Loop4 had no significant effect on the cell cycle of any cell line tested.

**3.5. Analysis of Expression Levels of the G<sub>1</sub> to S-Phase Regulators CDK4 and Cyclin D1 in the Host Cell Cycle Progression.** Given that PorA-Loop4 inhibits the host cell cycle by increasing the proportion of cells at the G<sub>1</sub> checkpoint, we investigated whether PorA-Loop4 treatment resulted in changes in expression of CDK4 and Cyclin D1 at the mRNA and protein levels. HBMECs were treated with PorA-Loop4 for up to 24 h, and RNA was extracted and analyzed by qRT-PCR. Treatment with PorA-Loop4 peptide resulted in increased levels of CDK4 mRNA and decreased levels of Cyclin D1 mRNA (Figure 5(a)). In parallel, cells treated with PorA-Loop4 for 24 h and untreated control cells were lysed for immunoblotting and densitometry analysis. In line with the RNA analysis, levels of phosphorylated CDK4 (p-CDK4) were significantly increased, while levels of Cyclin D1 were significantly reduced in treated cells (Figure 5(b)).

To determine whether the effects of PorA-Loop4 on p-CDK4 and Cyclin D1 on treated cells were reflected during interactions between whole meningococci and HBMECs, and whether this effect could be demonstrated to be mediated by the presence of the surface loop 4, HBMECs were infected with wild-type *N. meningitidis* strain MC58 or its

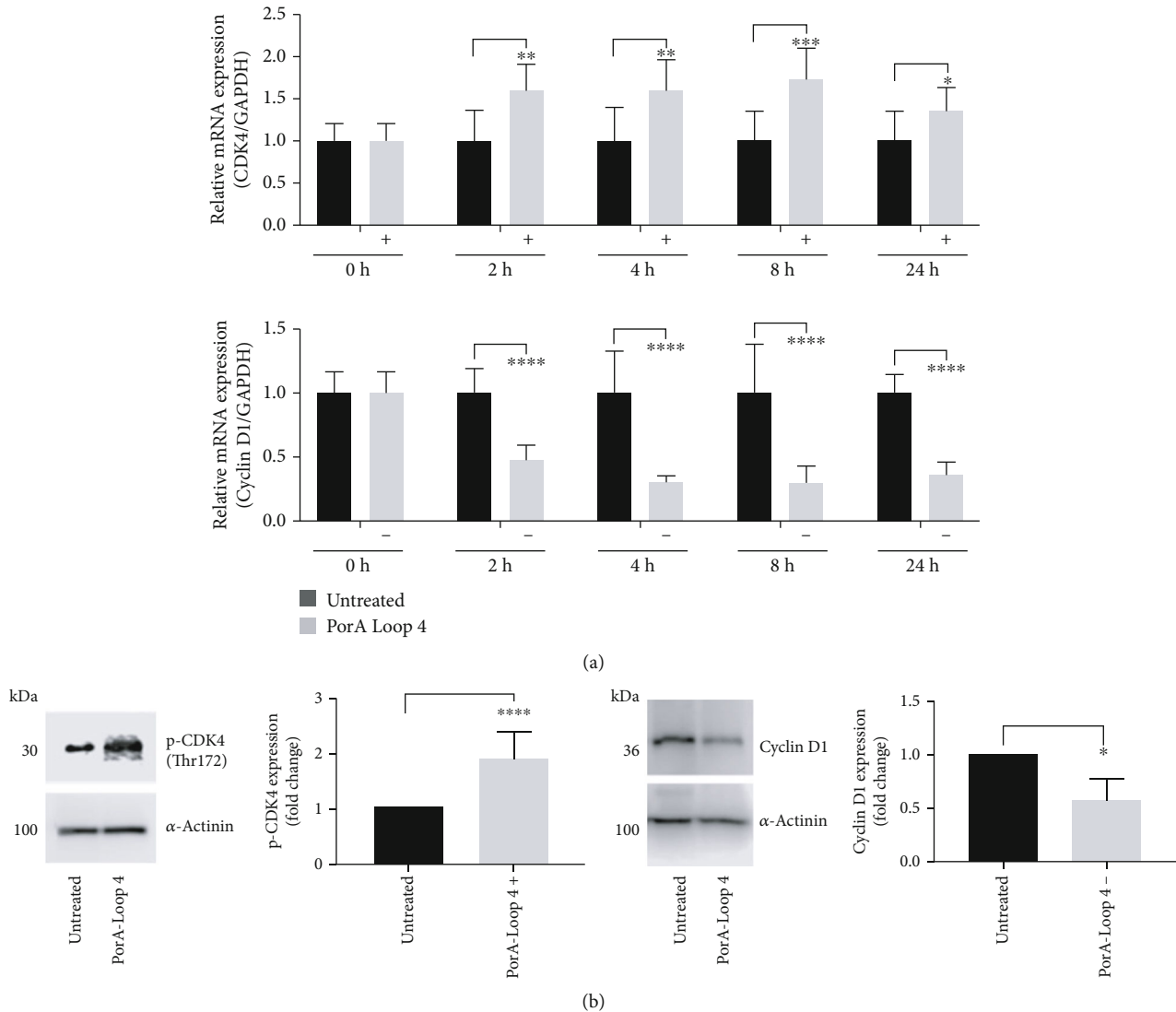


FIGURE 5: PorA-Loop4 peptide cause an increased expression of CDK4 and decreased expression of Cyclin D1 both at the mRNA and protein level. (a) HBMECs were either left untreated or treated with PorA-Loop4 (50  $\mu$ M) for up to 24 h. RNA was extracted, cDNA was generated, and qRT-PCR was performed to analyze the mRNA expression of CDK4 and Cyclin D1. Bars represent the expression ( $2^{-\Delta\Delta C_T}$ , fold change) of CDK4 and Cyclin D1 relative to GAPDH levels as the housekeeping gene. Data were normalized to the untreated cells. (b) The treated (24 h) and untreated HBMECs were collected and lysed for immunoblotting and densitometry analysis of p-CDK4 (Thr172)/Cyclin D1 protein expression. Alpha actinin was used to normalize protein loading. The figure shows a representative blot with lanes from different areas of the same membrane. Band intensities were quantified by densitometric analysis using Image J and normalized to alpha actinin. qRT-PCR and immunoblotting were each performed in three independent experiments. Significant difference to the untreated (\* $P \leq 0.05$ , \*\* $P \leq 0.01$ , \*\*\* $P \leq 0.001$ , and \*\*\*\* $P \leq 0.0001$ ), *t*-test.

derivative expressing a mutant PorA lacking loop 4 (MC58  $\Delta$ PorA-Loop4) for 8 h, and levels of p-CDK4 and Cyclin D1 were determined by immunoblotting and densitometry after lysis of the cells. Expression of p-CDK4 was significantly increased in cells infected with wild-type meningococci, in contrast to cells treated with the loop 4 deletion mutant, where levels of this protein were not significantly different to those in untreated cells (Figure 6(a)). Furthermore, the expression of Cyclin D1 was significantly lower in cells infected with wild-type meningococci compared to uninfected cells after 8 h infection (Figure 6(b)). Levels of Cyclin D1 in cells treated with the loop 4 deletion mutant

were increased compared to untreated cells, suggesting that interactions between the meningococci and HBMECs that were independent of PorA-Loop4 also affected levels of Cyclin D1, but this effect was suppressed in the presence of loop 4. The findings of the immunoblotting experiments were confirmed by confocal microscopy. HBMEC monolayers infected with wild-type meningococci exhibited higher levels of p-CDK4 (Figure 7) and lower levels of Cyclin D1 (Figure 8) compared to uninfected cells, while cells infected with the isogenic mutant lacking loop 4 displayed similar levels of p-CDK4 to uninfected cells (Figure 7) and slightly higher levels of Cyclin D1 (Figure 8).

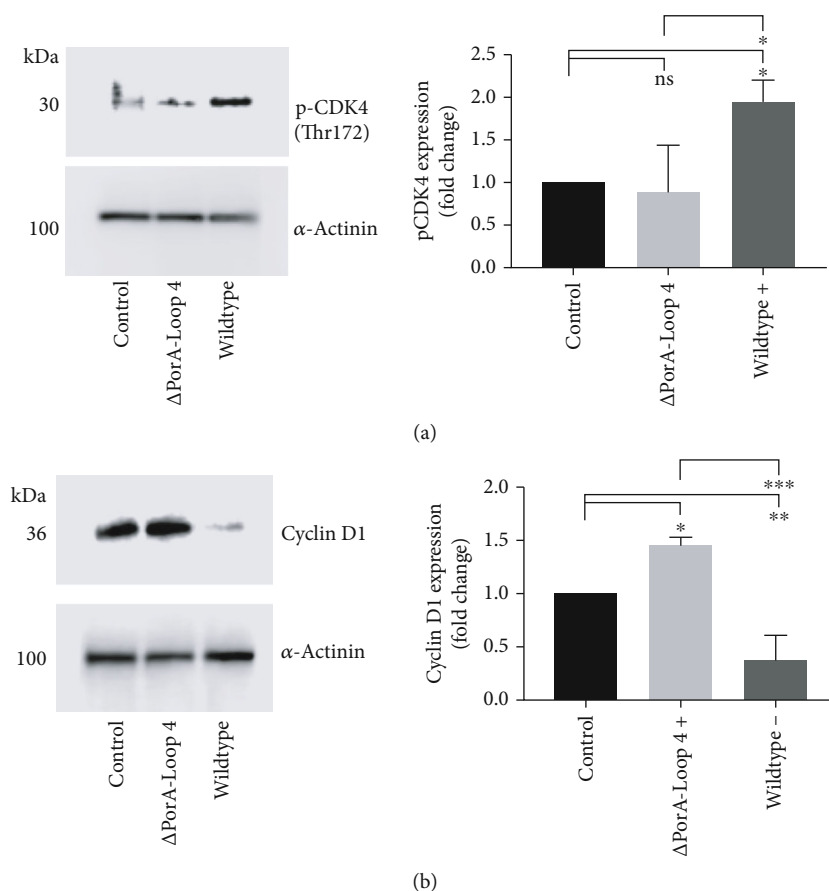


FIGURE 6: Infection of HBMECs with *N. meningitidis* MC58 and  $\Delta$ PorA-Loop4 causes perturbations in p-CDK4 (Thr172) and Cyclin D1 expression. HBMECs were left uninfected (control) or infected with wild-type *N. meningitidis* MC58 or its isogenic derivative MC58  $\Delta$ PorA-Loop4 at MOI 500 for 8 h, 37°C, and 5% CO<sub>2</sub>. Cells were lysed for immunoblotting and densitometry analysis of p-CDK4 (Thr172) (a) and Cyclin D1 (b) protein expression. Alpha actinin was used to normalize protein loading. The figure shows a representative blot with lanes from different areas of the same membrane (left). Band intensities were quantified by densitometric analysis using Image J and normalized to alpha actinin (right). Immunoblotting was each performed in three independent experiments. Significant difference to the untreated (\* $P \leq 0.05$ , \*\* $P \leq 0.01$ , and \*\*\* $P \leq 0.001$ , ns: not significant), ANOVA (with Tukey's test applied post hoc).

#### 4. Discussion

The human laminin receptor is a well-documented ligand for several important human pathogens, and LamR has been implicated in the cell surface binding and adhesion of meningococci, *Haemophilus influenzae*, and *Streptococcus pneumoniae*. Interaction of meningococci with LamR is mediated by the outer membrane proteins PorA and PilQ; the porin PorA interacts with LamR through its fourth extracellular loop, and this activity was further mapped to residues 192-208 of PorA [5, 21]. Here, we have shown that the interaction of this region of PorA with LamR is mediated through the 37LRP form of the receptor, and that it mediates important host cell responses including inhibition of bacterial cellular invasion, epithelial cell migration, and a G<sub>1</sub> cell cycle arrest in epithelial and endothelial cells.

The structure of porins is conserved across many Gram-negative bacteria and is characterized by the presence of membrane-spanning beta sheets separated by surface-exposed loops, some of which have been shown to interact with host cells [27]. Several studies have shown that individ-

ual extracellular loops are utilized by pathogens to exploit binding and signalling during adhesion and internalization. Vitiello et al. [28] examined the role of *H. influenzae* (type B) porin P2 and its active peptide, Loop L7. Similarly, the entry of *Escherichia coli* into HBMEC cells was mediated by loops 1, 2, and 3 of the porin OmpA via the host receptor cPLA2  $\alpha$  [29]. More recently, Kattner et al. [11] showed that mutations in the extracellular loops of PorB in a serogroup W *N. meningitidis* isolate significantly reduced TLR2-dependent activity, indicating that loop 7 of this porin mediates the binding to TLR2.

We showed that while meningococci colocalize with both forms of LamR, significantly less 37LRP was recruited to colonies of a mutant strain lacking PorA Loop4 compared to its wild-type parent, while colocalization with 67LR was unaffected. This is in line with previously published data where we observed reduced binding to recombinant LamR by an *N. meningitidis* MC58  $\Delta$ PorA mutant [5]. This was extended to investigate the role of the different receptors on the ability of the meningococcus to invade an endothelial monolayer. Previously, we showed that siRNA knockdown

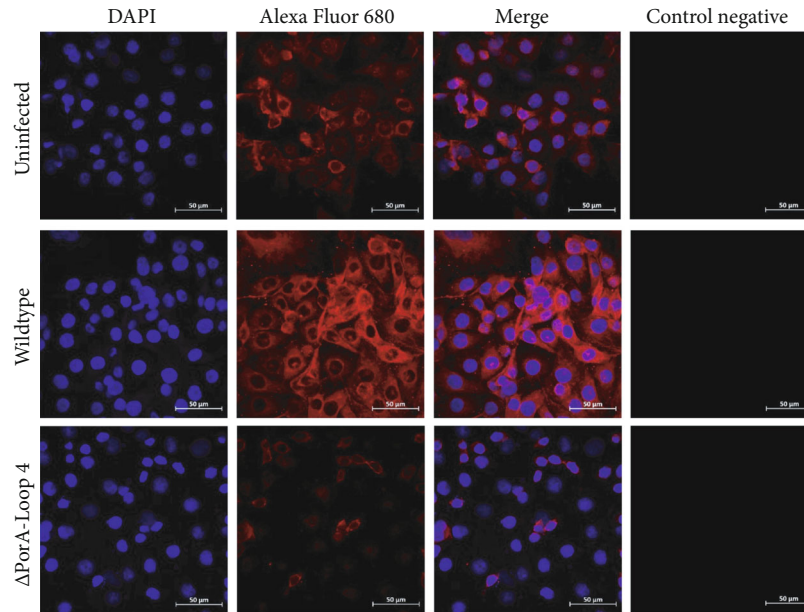


FIGURE 7: Localization of p-CDK4 in infected HBMECs. HBMECs were left uninfected or were infected with wild-type *N. meningitidis* MC58 or its isogenic derivative MC58  $\Delta$ PorA-Loop4 at MOI 500 for 8 h, 37°C, and 5% CO<sub>2</sub>. Cells were fixed with 4% paraformaldehyde and stained with anti-p-CDK4 (1 : 500) overnight, followed by secondary Alexa antibody (Alexa Fluor 680, red) overnight. Primary antibody was omitted in control images. Merged images also show DAPI staining (blue). Coverslips were mounted using ProLong Gold antifade mounting reagent. Scale bar = 50  $\mu$ m. Images representative of at least 3 independent experiments.

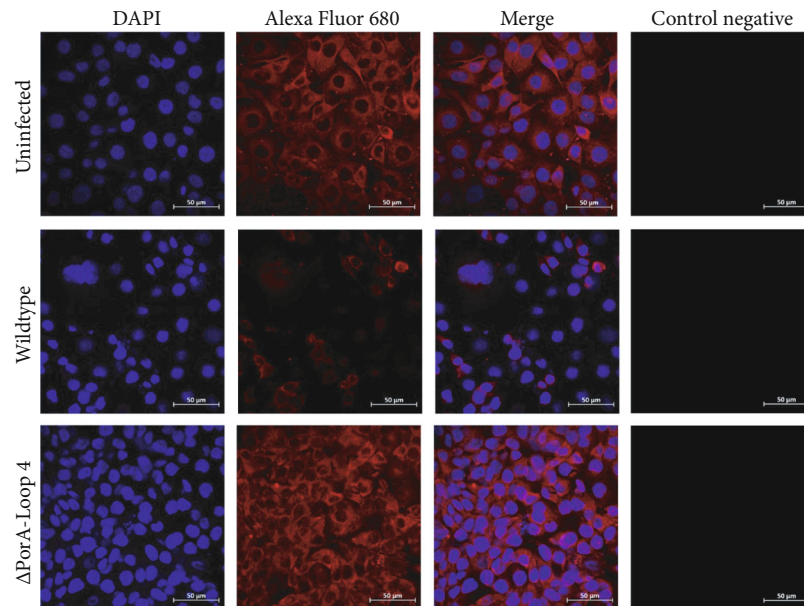


FIGURE 8: Localization of Cyclin D1 in infected HBMECs. HBMECs were left uninfected or were infected with wild-type *N. meningitidis* MC58 or its isogenic derivative MC58  $\Delta$ PorA-Loop4 at MOI 500 for 8 h, 37°C, and 5% CO<sub>2</sub>. Cells were fixed with 4% paraformaldehyde and stained with anti-Cyclin D1 (1 : 500) overnight, followed by secondary Alexa antibody (Alexa Fluor 680, red) overnight. Primary antibody was omitted in control images. Merged images also show DAPI staining (blue). Coverslips were mounted using ProLong Gold antifade mounting reagent. Scale bar = 50  $\mu$ m. Images representative of at least 3 independent experiments.

of the LamR gene, *RPSA*, in HBMECs reduced surface expression of 37LRP but not 67LR after 12 h of treatment [30]. Here, we showed using siRNA knockdown of *RPSA* in HBMECs that reduction of the surface expression of 37LRP significantly reduced the ability of meningococci to invade these cells. Sim-

ilarly, the use of blocking antibodies specific for either 37LRP or 67LR showed that cellular invasion was promoted by interaction with 37LRP but not with 67LR.

There is growing evidence (in line with this study) that suggests 67LR is predominantly a substrate-dependent

molecule whereas 37LRP represents a transient, more dynamic species. Kim et al. [31] identified a cellular laminin receptor binding partner known as lysyl-tRNA synthetase. This protein translocates to the membrane after binding to a substrate (such as laminin or collagen) initiating phosphorylation and subsequent association with 67LR. This was shown to protect 67LR from Nedd4-mediated ubiquitination and subsequent degradation. This may explain why 67LR is resistant to LamR siRNA targeting over a relatively short time in cells growing on a substrate by stabilizing this molecule and thus decreasing its turnover.

The laminin receptor is well established as a multifunctional protein with important roles in cellular adhesion, protein translation, and interactions with numerous pathogens. While the precursor-product relationship between 37LRP and 67LR is widely accepted, the mechanism driving 67LR formation remains unresolved. Here, we confirm previous evidence of distinct surface populations of 37LRP and 67LR with potentially important functional consequences for pathogen-host cell interactions.

For *N. meningitidis*, the epithelium represents an important physical barrier against invasion, and the organism has been shown to target various surface receptors on epithelial cells. These include alpha actinin [32], integrins [33–35], carcinoembryonic antigen-related cell adhesion molecules (CEACAMs) [36, 37], CD46 [38, 39], platelet-activating factor receptor [40], galectin-3 [41], various receptor tyrosine kinases [42–44] (including fibroblast growth factor receptor 1-IIIc, which is specific for the microvasculature of the blood-brain barrier [44]), and the laminin receptor [5]. In addition to protein receptors, the meningococcus has recently been shown to target the plasma membrane sphingolipids globotriaosylceramide (Gb3) and raft-associated monosialotetrahexosylganglioside (GM1) [45]. Given the ability of meningococci to disrupt epithelial layers, the laminin receptor's role as a cellular receptor, and the identification of the PorA-LamR interaction as playing an important role in host cell fate, we hypothesized that meningococci would be able to modulate the integrity of the monolayer via the interaction between these molecules. We tested this by investigating the ability of PorA-Loop4 to inhibit wound healing. Wound healing of epithelial cell monolayers was significantly inhibited by PorA-Loop4 over a 16- and 60-hour time period. This effect was cytostatic and rather than cytotoxic, as has been observed in other pathogenic bacteria, which are able to inhibit wound concomitantly with cytotoxic effects including cell rounding and detachment at the wound edge [46]. Recently, disease-associated meningococci were shown to inhibit wound healing in epithelial cells *in vitro* [24]. The bacterial component responsible for this effect was not determined, but it was shown to be independent of type IV pili and several other surface structures including the capsular polysaccharide. This demonstrates that intact meningococci inhibit wound healing and that this effect is not limited to the peptide used in our study, while our findings suggest a mechanism for the observations described by Ren and MacKichan [24]. While wound healing can result from cell proliferation as well as cell migration, closure of a wounded monolayer within the first 24 hours

has been shown previously to result primarily from cell migration [47]. In our experiments, we employed HCT116 cells, which are reported to have a doubling time of approximately 18 hours [48]. Therefore, as the wound area was approximately 25 cell bodies wide and the wound was largely closed by 24 hours, only migration could account for the observed wound healing at the earlier timepoints. At the later timepoints of 40 and 60 hours, it is possible that cell proliferation may also contribute to the observed wound healing, and this would be consistent with our observed cell cycle arrest.

The role of LamR, and particularly 37LRP, in regulation of the host cell cycle has been documented previously in both yeast cells and mammalian cell models [49]. 37LRP is essential for viability of HeLa and Hep3b epithelial cells [50, 51], and siRNA knockdown of LamR inhibited proliferation via a G<sub>1</sub> cell cycle arrest in HT1080 epithelial cells [26]. To investigate whether inhibition of cell migration was due to an anti-proliferation effect, we looked at DNA synthesis in epithelial and endothelial cell lines. The host cell cycle is a tightly controlled process mediated by major regulatory molecules known as cyclin-dependent kinases (CDKs) and cyclins. During cell cycle progression, cyclins accumulate during interphase and are rapidly degraded during late mitosis. CDK4 and Cyclin D1 bind to form the first cyclin complex and control the transition from G<sub>1</sub> to S-phase. Different CDK-cyclin complexes regulate each checkpoint of the cell cycle based on upstream signalling events. Here, we show that PorA-Loop4 treatment caused a G<sub>1</sub> cell cycle arrest in epithelial and endothelial cells. The G<sub>1</sub> arrest we observed in HBMECs was accompanied by decreased expression Cyclin D1 and increased expression of CDK4, both at the mRNA and protein levels. This suggests that the change in mRNA levels strongly correlate with change in protein levels, and we could propose that the regulation of gene expression of Cyclin D1 and CDK4 is tightly controlled upstream of translation. The wild-type-infected HBMECs showed similar perturbation of CDK4/Cyclin D1 to the treated Loop4 samples, while treatment with the mutant lacking PorA-Loop4 had the opposite effect.

The potential for meningococci to cause cell cycle arrest was also suggested by previous studies. Von Papen et al. confirmed that meningococcal infection arrested the cycle of epithelial cells (Detroit 562 and NP69) in G<sub>1</sub> phase at 24 h postinfection, while in parallel, a significant decrease of cells in the S-phase was observed [52]. They observed by immunoblotting that bacterial infection resulted in a decreased protein expression of Cyclin D1 and an increase of Cyclin E. Interestingly, another study found that the outer membrane opacity proteins (Opa) caused S-phase arrest via p21 and cyclin G<sub>2</sub> in human brain endothelial cells [53]. Thus, it appears that meningococci can influence the host cell cycle at multiple points via different bacterial/host cell protein interactions.

A transcriptional study reported changes in HBMEC gene expression in response to meningococcal infection [54]. At least a two-fold increase in Cyclin D1, Cyclin D3, and CDKs 8 and 9 were reported after four hours of infection, indicating significant changes to the key cell cycle

control molecules at the G<sub>1</sub> checkpoint in response to infection. Interestingly, they also confirmed a decrease in the expression of LamR mRNA at 4- and 8-hour postinfection. While this does not confirm the population of laminin receptor molecules on the cell surface, it is interesting to note that expression is affected by infection.

Other pathogens have been shown to manipulate the cell cycle as a strategy to colonize and infect a host cell. Indeed, the closely related human pathogen *N. gonorrhoeae* has been shown to modulate the cell cycle via a G<sub>1</sub> cell cycle arrest (through decreased levels of Cyclin D1) [55], and gonococci interfere with the host cell cycle via translocation of bacterial restriction endonucleases into the host cell nucleus where they cause double strand breaks in the DNA and thus prevent progression of the host cell cycle [56]. We propose that meningococci subvert host cell processes to facilitate long term colonization rather than pathogenesis. Such manipulation of the host cell, however, would clearly have implications for pathogenesis by preventing or reducing normal cellular responses at the site of colonization. It was shown recently that G<sub>1</sub> cell cycle arrest (induced by serum starvation) led to an increase in GM1 molecules in the plasma membrane [45]. This in turn led to increased bacterial invasion, suggesting a mechanism by which engagement of LamR can promote invasion by meningococci and other pathogens targeting the blood brain barrier. It should also be noted that PorA is present not only on the meningococcal surface but also on membrane blebs, which are released in large amounts by growing meningococci [57, 58]. PorA-Loop4:37LRP interaction with cells in the local microenvironment is likely to influence normal turnover and renewal of epithelium or endothelium by stalling the cell cycle and ultimately allowing bacteria to initiate a sustained colonization.

The laminin receptor is the source of intense research activity with regard to tumor development, metastasis, and cancer therapy, as well as other pathological conditions such as Alzheimer's disease [59]. There is also growing evidence to suggest the laminin receptor represents an important receptor for a range of viral and bacterial pathogens. Here, we provide mechanistic insight into the LamR-mediated interaction of meningococci with host cells that have important implications for both infection and possibly other pathologies. Future studies will focus on gaining a full understanding of the control of the cell cycle mechanism and its role in the meningococcal interaction. It will be important to further elucidate the signalling pathway responsible for eliciting cell cycle arrest in epithelial and endothelial cells from the membrane to the nucleus to better understand the mechanism of host cell subversion by the meningococcus.

## Data Availability

Data are available upon requests.

## Disclosure

Matthew Vassey's permanent address is College of Health and Life Sciences, Aston University, Birmingham, UK. Rininta Firdaus's permanent address is Department of Bio-

materials, Institute of Clinical Science, Sahlgrenska Academy, University of Gothenburg, Sweden. Akhmed Aslam's permanent address is Faculty of Applied Medical Sciences, Umm Al-Qura University, Makkah, Saudi Arabia. Ala'Aldeen's permanent address is Middle East Research Institute, Erbil, Kurdistan Region of Iraq. The funders had no role in study design, data collection and analysis, decision to publish, or preparation of the manuscript.

## Conflicts of Interest

The authors declare that they have no conflicts of interest.

## Authors' Contributions

Matthew Vassey and Rininta Firdaus contributed equally to this work. Rininta Firdaus is the joint first author.

## Acknowledgments

The authors thank Dr. Abouseada for providing the meningococcal strains used in this study. This work was funded by the Medical Research Council, UK (<http://www.mrc.ac.uk>); award number G0801173.

## Supplementary Materials

Supplementary Table S1 presents data showing significant increases in PorA-Loop4-treated Detroit 526 and HCT116 cells in G<sub>1</sub> phase compared to untreated cells (comparable data for HBMECs presented in Figure 4). Supplementary Figure S1 shows a confocal image demonstrating the distribution of the two forms of laminin receptor (37LRP and 67LR) on uninfected HBMEC cells. Supplementary Figure S2 shows an immunoblot confirming that the  $\Delta$ PorA mutant strain expressed no PorA protein, while the  $\Delta$ PorA-Loop4 mutant expressed a mutant form of PorA lacking its fourth extracellular loop. Supplementary Figure S3 shows demonstrating that recruitment of 67LR is unaffected by deletion of PorA-Loop4 but the ability of this mutant to recruit 37LRP was significantly reduced. The data shows colocalization data obtained by confocal microscopy expressed as a histogram. Supplementary Figure S4 shows that treatment of D562 cells treated with PorA-Loop4 results in a lower proportion of these cells entering S-phase (comparable to data shown for HCT116 cells in Figure 3). (*Supplementary Materials*)

## References

- [1] L. V. Hooper, "Do symbiotic bacteria subvert host immunity?," *Nature Reviews Microbiology*, vol. 7, no. 5, pp. 367–374, 2009.
- [2] J. Benz and A. Meinhart, "Antibacterial effector/immunity systems: it's just the tip of the iceberg," *Current Opinion in Microbiology*, vol. 17, pp. 1–10, 2014.
- [3] S. Galdiero, A. Falanga, M. Cantisani et al., "Microbe-host interactions: structure and role of gram-negative bacterial porins," *Current Protein & Peptide Science*, vol. 13, no. 8, pp. 843–854, 2012.

- [4] P. Massari, S. Ram, H. Macleod, and L. M. Wetzler, "The role of porins in neisserial pathogenesis and immunity," *Trends in Microbiology*, vol. 11, no. 2, pp. 87–93, 2003.
- [5] C. J. Orihuela, J. Mahdavi, J. Thornton et al., "Laminin receptor initiates bacterial contact with the blood brain barrier in experimental meningitis models," *The Journal of Clinical Investigation*, vol. 119, no. 6, pp. 1638–1646, 2009.
- [6] K. V. Lithgow, B. Church, A. Gomez et al., "Identification of the neuroinvasive pathogen host target, LamR, as an endothelial receptor for the *Treponema pallidum* adhesin Tp0751," *mSphere*, vol. 5, no. 2, 2020.
- [7] S. Zhou, X. He, C. Xu et al., "The outer membrane protein P2 (OmpP2) of *Haemophilus parasuis* induces proinflammatory cytokine mRNA expression in porcine alveolar macrophages," *Veterinary Journal*, vol. 199, no. 3, pp. 461–464, 2014.
- [8] H. Nikaido, "Molecular basis of bacterial outer membrane permeability revisited," *Microbiology and Molecular Biology Reviews*, vol. 67, no. 4, pp. 593–656, 2003.
- [9] M. Cantisani, M. Vitiello, A. Falanga, E. Finamore, M. Galdiero, and S. Galdiero, "Peptides complementary to the active loop of porin P2 from *Haemophilus influenzae* modulate its activity," *International Journal of Nanomedicine*, vol. 7, pp. 2361–2371, 2012.
- [10] M. Galdiero, M. Vitiello, E. Sanzari et al., "Porins from *Salmonella enterica* serovar typhimurium activate the transcription factors activating protein 1 and NF-kappaB through the Raf-1-mitogen-activated protein kinase cascade," *Infection and Immunity*, vol. 70, no. 2, pp. 558–568, 2002.
- [11] C. Kattner, D. N. Toussi, J. Zaucha et al., "Crystallographic analysis of *Neisseria meningitidis* PorB extracellular loops potentially implicated in TLR2 recognition," *Journal of Structural Biology*, vol. 185, no. 3, pp. 440–447, 2014.
- [12] D. N. Toussi, L. M. Wetzler, X. Liu, and P. Massari, "*Neisseriae* internalization by epithelial cells is enhanced by TLR2 stimulation," *Microbes and infection/Institut Pasteur*, vol. 18, no. 10, pp. 627–638, 2016.
- [13] Y. Zhou, S. Feng, X. He et al., "Surface-exposed loops L7 and L8 of *Haemophilus (Glaesserella) parasuis* OmpP2 contribute to the expression of proinflammatory cytokines in porcine alveolar macrophages," *Veterinary Research*, vol. 50, no. 1, p. 105, 2019.
- [14] S. Galdiero, D. Capasso, M. Vitiello, M. D'Isanto, C. Pedone, and M. Galdiero, "Role of surface-exposed loops of *Haemophilus influenzae* protein P2 in the mitogen-activated protein kinase cascade," *Infection and Immunity*, vol. 71, no. 5, pp. 2798–2809, 2003.
- [15] V. Severino, A. Chambery, M. Vitiello et al., "Proteomic analysis of human U937 cell line activation mediated by *Haemophilus influenzae* type b P2 porin and its surface-exposed loop 7," *Journal of Proteome Research*, vol. 9, no. 2, pp. 1050–1062, 2010.
- [16] M. Vitiello, S. Galdiero, M. D'Isanto et al., "Pathophysiological changes of gram-negative bacterial infection can be reproduced by a synthetic peptide mimicking loop L7 sequence of *Haemophilus influenzae* porin," *Microbes and Infection/Institut Pasteur*, vol. 10, no. 6, pp. 657–663, 2008.
- [17] M. C. Maiden and I. M. Feavers, "Meningococcal typing," *Journal of Medical microbiology*, vol. 40, no. 3, pp. 157–158, 1994.
- [18] M. C. Maiden, J. Suker, A. J. McKenna, J. A. Bygraves, and I. M. Feavers, "Comparison of the class 1 outer membrane proteins of eight serological reference strains of *Neisseria meningitidis*," *Molecular Microbiology*, vol. 5, no. 3, pp. 727–736, 1991.
- [19] C. Brehony, K. A. Jolley, and M. C. Maiden, "Multilocus sequence typing for global surveillance of meningococcal disease," *FEMS Microbiology Reviews*, vol. 31, no. 1, pp. 15–26, 2007.
- [20] J. E. Russell, K. A. Jolley, I. M. Feavers, M. C. Maiden, and J. Suker, "PorA variable regions of *Neisseria meningitidis*," *Emerging Infectious Diseases*, vol. 10, no. 4, pp. 674–678, 2004.
- [21] N. M. Abouseada, M. S. Assafi, J. Mahdavi et al., "Mapping the laminin receptor binding domains of *Neisseria meningitidis* PorA and *Haemophilus influenzae* OmpP2," *PLoS One*, vol. 7, no. 9, article e46233, 2012.
- [22] N. J. Oldfield, S. J. Bland, M. Taraktoglou et al., "T-cell stimulating protein A (TspA) of *Neisseria meningitidis* is required for optimal adhesion to human cells," *Cellular Microbiology*, vol. 9, no. 2, pp. 463–478, 2007.
- [23] T. Takahashi, R. S. Nowakowski, and V. S. Caviness Jr., "BUdR as an S-phase marker for quantitative studies of cytokinetic behaviour in the murine cerebral ventricular zone," *Journal of Neurocytology*, vol. 21, no. 3, pp. 185–197, 1992.
- [24] X. Ren and J. K. MacKichan, "Disease-associated *Neisseria meningitidis* isolates inhibit wound repair in respiratory epithelial cells in a type IV pilus-independent manner," *Infection and Immunity*, vol. 82, no. 12, pp. 5023–5034, 2014.
- [25] K. J. Livak and T. D. Schmittgen, "Analysis of relative gene expression data using real-time quantitative PCR and the  $2^{-\Delta\Delta C_T}$  method," *Methods*, vol. 25, no. 4, pp. 402–408, 2001.
- [26] J. Scheiman, J. C. Tseng, Y. Zheng, and D. Meruelo, "Multiple functions of the 37/67-kd laminin receptor make it a suitable target for novel cancer gene therapy," *Molecular Therapy*, vol. 18, no. 1, pp. 63–74, 2010.
- [27] R. Koebnik, K. P. Locher, and P. Van Gelder, "Structure and function of bacterial outer membrane proteins: barrels in a nutshell," *Molecular Microbiology*, vol. 37, no. 2, pp. 239–253, 2000.
- [28] M. Vitiello, E. Finamore, M. Cantisani et al., "P2 porin and loop L7 from *Haemophilus influenzae* modulate expression of IL-6 and adhesion molecules in astrocytes," *Microbiology and Immunology*, vol. 55, no. 5, pp. 347–356, 2011.
- [29] R. Maruvada and K. S. Kim, "Extracellular loops of the *Escherichia coli* outer membrane protein A contribute to the pathogenesis of meningitis," *The Journal of Infectious Diseases*, vol. 203, no. 1, pp. 131–140, 2011.
- [30] F. Alqahtani, J. Mahdavi, L. M. Wheldon et al., "Deciphering the complex three-way interaction between the non-integrin laminin receptor, galectin-3 and *Neisseria meningitidis*," *Open Biology*, vol. 4, no. 10, 2014.
- [31] D. G. Kim, J. W. Choi, J. Y. Lee et al., "Interaction of two translational components, lysyl-tRNA synthetase and p40/37LRP, in plasma membrane promotes laminin-dependent cell migration," *FASEB Journal*, vol. 26, no. 10, pp. 4142–4159, 2012.
- [32] E. C. C. Sa, N. J. Griffiths, I. Murillo, and M. Virji, "*Neisseria meningitidis* Opc invasin binds to the cytoskeletal protein  $\alpha$ -actinin," *Cellular Microbiology*, vol. 11, no. 3, pp. 389–405, 2009.
- [33] O. Sokolova, N. Heppel, R. Jagerhuber et al., "Interaction of *Neisseria meningitidis* with human brain microvascular endothelial cells: role of MAP- and tyrosine kinases in invasion and inflammatory cytokine release," *Cellular Microbiology*, vol. 6, no. 12, pp. 1153–1166, 2004.

- [34] H. Slanina, A. Konig, S. Hebling, C. R. Hauck, M. Frosch, and A. Schubert-Unkmeir, "Entry of *Neisseria meningitidis* into mammalian cells requires the Src family protein tyrosine kinases," *Infection and Immunity*, vol. 78, no. 5, pp. 1905–1914, 2010.
- [35] H. Slanina, S. Hebling, C. R. Hauck, and A. Schubert-Unkmeir, "Cell invasion by *Neisseria meningitidis* requires a functional interplay between the focal adhesion kinase, Src and cortactin," *PLoS One*, vol. 7, no. 6, article e39613, 2012.
- [36] P. Muenzner, C. Dehio, T. Fujiwara, M. Achtman, T. F. Meyer, and S. D. Gray-Owen, "Carcinoembryonic antigen family receptor specificity of *Neisseria meningitidis* Opa variants influences adherence to and invasion of proinflammatory cytokine-activated endothelial cells," *Infection and Immunity*, vol. 68, no. 6, pp. 3601–3607, 2000.
- [37] M. Virji, K. Makepeace, D. J. Ferguson, and S. M. Watt, "Carcinoembryonic antigens (CD66) on epithelial cells and neutrophils are receptors for Opa proteins of pathogenic neisseriae," *Molecular Microbiology*, vol. 22, no. 5, pp. 941–950, 1996.
- [38] H. Kallstrom, M. K. Liszewski, J. P. Atkinson, and A. B. Jonsson, "Membrane cofactor protein (MCP or CD46) is a cellular pilus receptor for pathogenic *Neisseria*," *Molecular Microbiology*, vol. 25, no. 4, pp. 639–647, 1997.
- [39] M. Kirchner, D. Heuer, and T. F. Meyer, "CD46-independent binding of neisserial type IV pili and the major pilus adhesin, PilC, to human epithelial cells," *Infection and immunity*, vol. 73, no. 5, pp. 3072–3082, 2005.
- [40] F. E. Jen, M. J. Warren, B. L. Schulz et al., "Dual pili post-translational modifications synergize to mediate meningococcal adherence to platelet activating factor receptor on human airway cells," *PLoS Pathogens*, vol. 9, no. 5, article e1003377, 2013.
- [41] P. Quattroni, Y. Li, D. Lucchesi et al., "Galectin-3 binds *Neisseria meningitidis* and increases interaction with phagocytic cells," *Cellular Microbiology*, vol. 14, no. 11, pp. 1657–1675, 2012.
- [42] H. Slanina, S. Mundlein, S. Hebling, and A. Schubert-Unkmeir, "Role of epidermal growth factor receptor signaling in the interaction of *Neisseria meningitidis* with endothelial cells," *Infection and Immunity*, vol. 82, no. 3, pp. 1243–1255, 2014.
- [43] I. Hoffmann, E. Eugene, X. Nassif, P. O. Couraud, and S. Bourdoulous, "Activation of ErbB2 receptor tyrosine kinase supports invasion of endothelial cells by *Neisseria meningitidis*," *Journal of Cell Biology*, vol. 155, no. 1, pp. 133–144, 2001.
- [44] S. Azimi, L. M. Wheldon, N. J. Oldfield, D. A. A. Ala'Aldeen, and K. G. Wooldridge, "A role for fibroblast growth factor receptor 1 in the pathogenesis of *Neisseria meningitidis*," *Microbial Pathogenesis*, vol. 149, article 104534, 2020.
- [45] J. Schlegel, S. Peters, S. Doose, A. Schubert-Unkmeir, and M. Sauer, "Super-resolution microscopy reveals local accumulation of plasma membrane gangliosides at *Neisseria meningitidis* invasion sites," *Frontiers in Cell and Development Biology*, vol. 7, p. 194, 2019.
- [46] T. K. Geiser, B. I. Kazmierczak, L. K. Garrity-Ryan, M. A. Matthay, and J. N. Engel, "*Pseudomonas aeruginosa* ExoT inhibits in vitro lung epithelial wound repair," *Cellular microbiology*, vol. 3, no. 4, pp. 223–236, 2001.
- [47] F. Kheradmand, H. G. Folkesson, L. Shum, R. Derynk, R. Pytela, and M. A. Matthay, "Transforming growth factor- $\alpha$  enhances alveolar epithelial cell repair in a new *in vitro* model," *The American Journal of Physiology*, vol. 267, 6, Part 1, pp. L728–L738, 1994.
- [48] C. Biogene, "HCT 116 cell line: creative biogene technology," 2022, <https://www.creative-biogene.com/support/hct-116-cell-line.html>.
- [49] M. Demianova, T. G. Formosa, and S. R. Ellis, "Yeast proteins related to the p40/laminin receptor precursor are essential components of the 40 S ribosomal subunit (\*)," *Journal of Biological Chemistry*, vol. 271, no. 19, pp. 11383–11391, 1996.
- [50] Y. Kaneda, K. Kinoshita, M. Sato et al., "The induction of apoptosis in HeLa cells by the loss of LBP-p40," *Cell Death & Differentiation*, vol. 5, no. 1, pp. 20–28, 1998.
- [51] T. Susantad and D. R. Smith, "siRNA-mediated silencing of the 37/67-kDa high affinity laminin receptor in Hep3B cells induces apoptosis," *Cellular & Molecular Biology Letters*, vol. 13, no. 3, pp. 452–464, 2008.
- [52] M. von Papen, W. F. Oosthuysen, J. Becam, H. Claus, and A. Schubert-Unkmeir, "Disease and carrier isolates of *Neisseria meningitidis* cause G1 cell cycle arrest in human epithelial cells," *Infection and Immunity*, vol. 84, no. 10, pp. 2758–2770, 2016.
- [53] A. Schubert-Unkmeir, O. Sokolova, U. Panzner, M. Eigenthaler, and M. Frosch, "Gene expression pattern in human brain endothelial cells in response to *Neisseria meningitidis*," *Infection and Immunity*, vol. 75, no. 2, pp. 899–914, 2007.
- [54] A. Schubert-Unkmeir, A. Schramm-Gluck, M. Frosch, and C. Schoen, "Transcriptome analyses in the interaction of *Neisseria meningitidis* with mammalian host cells," *Methods in Molecular Biology*, vol. 470, pp. 5–27, 2009.
- [55] A. Jones, A. B. Jonsson, and H. Aro, "*Neisseria gonorrhoeae* infection causes a G1 arrest in human epithelial cells," *FASEB Journal*, vol. 21, no. 2, pp. 345–355, 2007.
- [56] L. Weyler, M. Engelbrecht, M. Mata Forsberg et al., "Restriction endonucleases from invasive *Neisseria gonorrhoeae* cause double-strand breaks and distort mitosis in epithelial cells during infection," *PLoS One*, vol. 9, no. 12, article e114208, 2014.
- [57] J. X. Wheeler, C. Vipond, and I. M. Feavers, "Exploring the proteome of meningococcal outer membrane vesicle vaccines," *Proteomics Clinical Applications*, vol. 1, no. 9, pp. 1198–1210, 2007.
- [58] C. Vipond, J. X. Wheeler, C. Jones, I. M. Feavers, and J. Suker, "Characterization of the protein content of a meningococcal outer membrane vesicle vaccine by polyacrylamide gel electrophoresis and mass spectrometry," *Human Vaccines*, vol. 1, no. 2, pp. 80–84, 2005.
- [59] K. Jovanovic, C. J. Chetty, T. Khumalo et al., "Novel patented therapeutic approaches targeting the 37/67 kDa laminin receptor for treatment of cancer and Alzheimer's disease," *Expert Opinion on Therapeutic Patents*, vol. 25, no. 5, pp. 567–582, 2015.